Journal of Atmospheric and Solar-Terrestrial Physics 73 (2011) 760–770

Contents lists available at ScienceDirect

Journal of Atmospheric and Solar-Terrestrial Physics

journal homepage: www.elsevier.com/locate/jastp

Equatorial ionospheric responses in relation to the occurrence of main phase of intense geomagnetic storms in the local dusk sector

R. Hajra, S.K. Chakraborty *

Department of Physics, Raja Peary Mohan College, Uttarpara, Hooghly 712258, West Bengal, India

ARTICLE INFO

Article history:
Received 15 November 2010
Received in revised form
14 February 2011
Accepted 20 February 2011

Keywords:
Equatorial ionosphere
Ionospheric irregularities
Solar wind–magnetosphere interactions
Ionosphere–magnetosphere interactions

ABSTRACT

During five intense geomagnetic storms with main phases occurring around local dusk sector, equatorial ionosonde and electrojet data, VHF/UHF scintillation data of Calcutta, and several solar wind parameters are investigated to ascertain the polarity of prompt penetration electric field (PPEF). Abrupt increases in AE, ASY-H and/or sharp decreases in D_{st}/SYM-H with strong southward IMF B_z may symbolize eastward PPEF to equatorial latitude leading to evolution of density irregularities if the period is associated with arrival and sustenance of large magnetospheric shock compression. On the contrary, westward PPEF is more feasible if the shock reduces suddenly or fluctuates with small values.

1. Introduction

The equatorial ionosphere is the seat of many interesting phenomena among which the equatorial ionization anomaly (EIA) and intense form of irregularities in electron density are two most important features. Under quiet geomagnetic conditions, while the former occurs over a large part of the day and extends well into the evening hours, the irregularities in the electron density distribution develop over the magnetic equator mostly in the postsunset period (Booker and Wells, 1938; Cohen and Bowles, 1961; Farley et al., 1970; Woodman and LaHoz, 1976). The $\boldsymbol{E} \times \boldsymbol{B}$ vertical drift of plasma at the magnetic equator and subsequent diffusion along the geomagnetic field lines develop the EIA. The postsunset prereversal enhancement (PRE) of eastward electric field is an important contributor for generation of equatorial ionospheric irregularities (Farley et al., 1970; Kil et al., 2009, and references therein). The primary factor for both the events, the electric field ($\boldsymbol{E}$) is significantly perturbed during geomagnetic disturbances. The perturbation effect becomes vigorous near sunset due to the day-to-night conductivity gradient. The intricate modification of the electric field at different phases of the storms is mainly controlled by the relative contributions (Maruyama et al., 2005) of two disturbance components, (i) prompt penetration (PP) electric field of magnetospheric origin (Senior and Blanc, 1984; Spiro et al., 1988) and (ii) the field related to ionospheric disturbance dynamo (DD) (Blanc and Richmond, 1980). The electric field perturbation at the low latitudes due to DD is effective within 1 to few hours (Blanc and Richmond, 1980; Fejer and Scherliess, 1995) of increase in magnetic activity and persists throughout the storm period and even beyond. It has polarity opposite to that of the quiet time diurnal field pattern. On the other hand, the polarity of the relatively short-lived (~2–3 h) PP electric field (Jaggi and Wolf, 1973; Senior and Blanc, 1984) depends on the rapid and large changes in magnetospheric convection driven by interplanetary magnetic field (IMF). During local postsunset hours sudden increase in convection (undershielding condition) leads to PP of eastward electric field to equatorial latitudes, while sudden decrease in convection (overshielding condition) at the same local time sector may generate westward PP electric field (Fejer and Scherliess, 1995, 1997). Solar wind conditions that strongly modulate the energy transfer rate from the solar wind into the magnetosphere are suggested to be the contributing factors in the prompt ionospheric responses (Mannucci et al., 2008). The effects related to PP electric field offer the opportunity to investigate the solar wind–magnetosphere–ionosphere coupling processes.

A geomagnetic storm is normally assumed to have a commencement stage, a main/driving phase and a recovery phase. Due to the evolution of various driving mechanisms ionospheric responses at different phases of storm vary significantly. The usual PRE of the electric field in the postsunset period is modulated mostly by (i) the field related to PP in the early stage of the main phase and by (ii) the combined fields due to PP and DD origins at the later stages of the storms. Postsunset enhancement of eastward electric field near the magnetic equator leads to the height rise of the F-layer plasma and thereby providing favorable conditions for generation of irregularities through Rayleigh–Taylor instability mechanism, while reverse modulation

* Corresponding author. Tel.: +91 33 26649178.
E-mail address: skchak2003@yahoo.com (S.K. Chakraborty).

1364-6826/$ - see front matter © 2011 Elsevier Ltd. All rights reserved.
doi:10.1016/j.jastp.2011.02.014

of PRE may inhibit the irregularity processes. The irregularities commonly known as equatorial spread-F (ESF) are observed using various techniques—ionospheric scintillation is one of such methods to detect the irregularities of specific scale sizes. Scintillation causes amplitude and phase distortion, cycle slip, message error of the transionospheric communication/navigation signals. It is most severe in the 10° wide belt around EIA crest under quiet geomagnetic conditions (Knight and Finn, 1996).

Study of the phenomena of ESF/scintillation in the context of geomagnetic disturbances is one of the important space weather issues (Aarons et al., 1980; Alex and Rastogi, 1987; Becker-Guedes et al., 2004; Hajra et al., 2010, and references therein). The development of plasma density irregularity/ESF related to PP of eastward electric field stimulated by rapid increase in high latitude convection around local sunset hours was reported by several authors (Abdu et al., 2003, and references therein). Basu et al. (2001, 2010) reported preferential occurrence of strong irregularities associated with PP in the specific longitude sectors for which the early evening period corresponds to rapid changes in D_{st} larger than -50 nT/h in the developing phase of the intense storms. A less stringent criterion – rates of change in D_{st} larger than -5 nT/h for more than 2 h – for triggering of equatorial plasma density irregularities in the evening local time sector was advocated by Huang et al. (2002). Multi-station study of Tulasi Ram et al. (2008) confirmed the preferential ESF development in longitude sectors with local time corresponding to postsunset hours during main phase of the storms. The same was attributed to the PP of eastward electric fields at the low latitudes, which is symbolized by sudden increase in AE index and/or pronounced decrease in SYM-H. Though many studies on the storm induced changes of equatorial ionosphere in the main phase during local dusk sector have been reported, the variability of storm time responses and identification of the corresponding driving mechanisms still possesses serious uncertainty. More case studies involving several solar wind parameters are, therefore, needed for better understanding of various types of space weather events and to increase the prediction capability of the ionospheric responses.

In the present paper a systematic study on the ionospheric and interplanetary parameters during five intense (two very intense ($D_{st} < -200$ nT) and three intense (-200 nT $\le D_{st} < -100$ nT)) geomagnetic storms is presented in the context of observing postsunset spread-F near the magnetic equator and scintillation near the anomaly crest. The main phase of each storm – marked by sharp fall in D_{st}/SYM-H index – occurs around local sunset hours of high solar activity period (1980–1981 and 1989–1990). In the process of validating the criteria put forwarded by several workers for the generation of irregularities associated with PP of electric fields during main phase of storms in the local postsunset hours, attempts have been made to identify the stringent conditions necessary for evolution of specific polarity of storm related equatorial electric field perturbations and subsequent occurrence/inhibition of ESF/scintillation.

2. Data

Available amplitude scintillation data at VHF (136.11 MHz)/UHF (244 MHz) from satellites ETS-2 (130°E)/Fleet Sat Com (FSC) (73°E) recorded at the Ionosphere Field Station, Haringhata (geographic: longitude, 88.38°E; latitude, 22.58°N; dip: 32°N), University of Calcutta, are studied under the present investigation. Scintillation data are scaled according to the usual "third peak" method. The observing station, Calcutta, is situated virtually below the northern crest of the EIA and presents an excellent platform for observing equatorial phenomena. The 400 km subionospheric point of ETS-2 path is located at 21°N, 92.7°E (geographic), dip: 27°N and that of FSC is located at 21.1°N, 87.1°E (geographic), dip: 27°N. For information regarding ESF and virtual height of F-layer ($h'F$) ionosonde data, available at 1 h interval, from the equatorial stations, Kodaikanal (geographic: longitude 77.5°E, latitude 10.25°N, dip: 4°N) and Trivandrum (geographic: latitude, 8.29°N; longitude, 76.57°E; dip: 1.2°S) are used.

The magnetometer H-field data are obtained from the Indian Institute of Geomagnetism, Mumbai. The strength of equatorial electrojet (EEJ) is estimated using the method suggested by Chandra and Rastogi (1974). Accordingly, the hourly variations of the horizontal component of the geomagnetic field relative to its nighttime value at Alibag (ΔH_A) (geographic: latitude, 18.63°N; longitude, 72.87°E; dip: 23°N) are subtracted from the corresponding values at Trivandrum (ΔH_T) for the measurement of EEJ strength, ($\Delta H_T - \Delta H_A$). Trivandrum is an EEJ station while Alibag is located outside the EEJ belt.

The data on solar wind parameters such as plasma flow pressure/solar wind pressure (P_{sw}), solar wind speed (V_{sw}), interplanetary electric field (IEF) E_{sw} are downloaded from the database available with OMNI2. It contains the hourly mean values of the interplanetary magnetic field (IMF) and solar wind parameters measured by various spacecrafts (ISEE3, IMP8, etc.) near the earth's orbit. The convection time delay between locations of the spacecrafts and the magnetopause is estimated to be ~4 min on the average and the same is incorporated in the temporal evolutions of solar wind parameters.

The SYM-H (H-component of symmetric ring current), ASY-H (H-component of asymmetric ring current) indices, the auroral electrojet (AE) index available at 1 min interval and hourly D_{st} values published by the World Data Center, Kyoto, are also used.

Ion density data recorded through sun-synchronous Defense Meteorological Satellite Program (DMSP) satellites F8 and F9 are used in the study to have a global picture of the ionosphere at 840 km altitude. DMSP F9 has ascending and descending nodes at 0930 h LT (local time) and 2130 h LT while DMSP F8 has ascending and descending nodes at 0600 h LT and 1800 h LT, respectively.

In the present study the local time of main phase onset (MPO) is determined by the time of intensification of the storms as revealed through sharp fall in D_{st}/SYM-H indices after storm sudden commencement (SSC). It is sometimes coincident with or preceded by the magnetospheric shock intensification and abrupt southward turning of IMF B_z (Kumar et al., 2005). The local sunset times used for the present investigation refer to the subionospheric sunset time of ETS-2 path.

3. Results

3.1. Storm on January 20, 1989

Following SSC at 1659 h IST (Indian Standard Time (IST)= universal time (UT) +0530 h) on January 20, 1989, the main phase of the intense geomagnetic storm initiates around 1817 h IST, just before the local sunset (1824 h IST being the local subionospheric sunset time of ETS-2 path) (Fig. 1). The SSC is accompanied by large increase in SYM-H that is followed by abrupt decrease at the rate < -50 nT/h (Fig. 1e). The development of the storm through two-step growth of ring current is evident from the variation of SYM-H. It reaches the minimum value of -131 nT at 0000 h IST (1830 h UT). The data for AE index is not available for this event and there is gap in IMF B_z data for the period (Fig. 1c). The ASY-H index is reported to correlate well with IMF B_z and AE indices (Clauer and McPherron, 1980). It exhibits a sharp increase during the main phase occurring in the

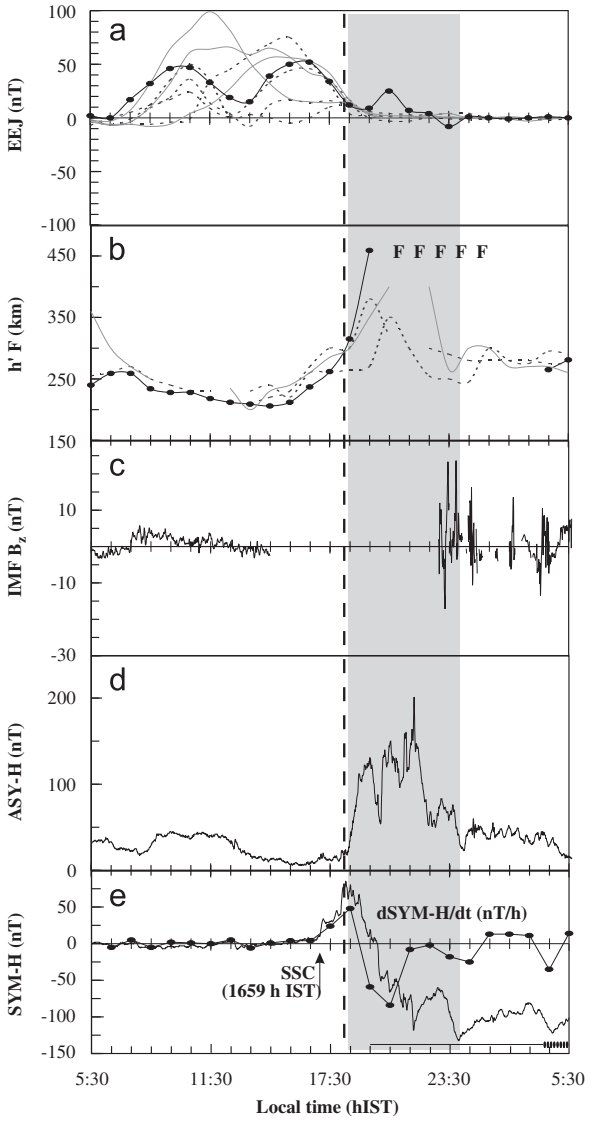

Fig. 1. Temporal variations of (a) equatorial electrojet EEJ (nT) (filled circles connected with bold lines) for the storm day along with mass plots of quiet days preceding and succeeding the storm day, the continuous and dotted lines pertaining to days with and without scintillation events, respectively, (b) $h'F$ (km) at an equatorial station, Trivandrum, for the storm day (filled circles connected with bold lines) along with diurnal variations during quiet days with (continuous lines) and without (dotted lines) scintillation events, (c) IMF B_z (nT), (d) ASY-H (nT), (e) SYM-H (nT) (continuous line) and dSYM-H/dt (nT/h) (filled circles connected by bold lines) for the storm event on January 20, 1989. In the panel (b) "F" denotes the occurrence of ESF at Trivandrum. The local time is expressed in Indian Standard Time (IST=UT+0530 h). The vertical dashed line represents the local time of onset of main phase (MPO) while local time of SSC is shown by a vertical arrow in panel (e). The shaded portion shows the time period after subionospheric sunset at ETS-2 satellite path till local midnight. The horizontal thick bar in the lower part of panel (e) represents the time periods of severe scintillation observations (SI > 10 dB) and vertical thick lines at the end indicate moderate scintillation with SI < 10 dB.

local dusk sector (Fig. 1d). Sastri et al. (1997) reported prompt upward plasma drift at the equatorial station, Kodaikanal, for asymmetric ring current development in the dusk sector. The diurnal variation of EEJ shows an unusual intensification after 1930 h IST compared to the normal variations of EEJ on neighboring quiet days (Fig. 1a). It may signify the PP of eastward electric field at the magnetic equator on the disturbed day, for on the magnetically quiet days no such unusual intensification is observed. In the $h'F$ data of equatorial station, Trivandrum,

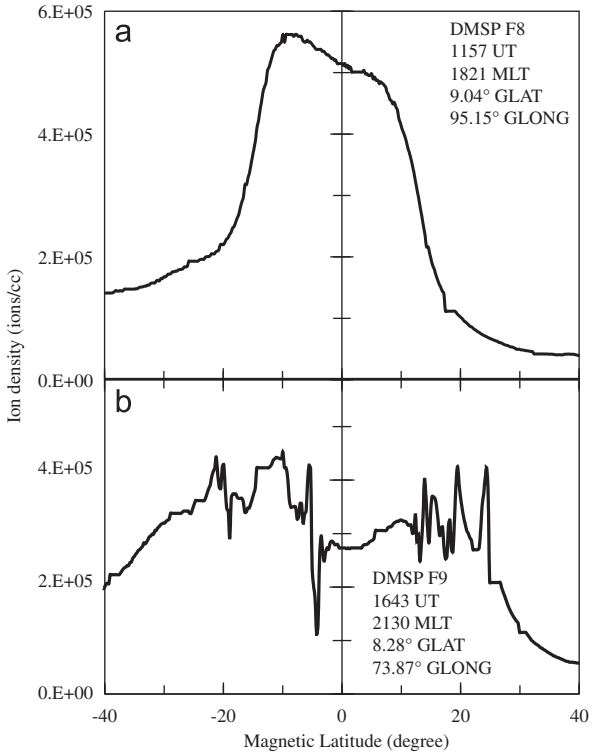

Fig. 2. Latitudinal variation of ion density (ions/cc) measured by (a) DMSP F8 and (b) DMSP F9 on January 20, 1989. The names of the spacecrafts and the corresponding magnetic equator crossing universal time (UT), magnetic local time (MLT), geographic latitude (GLAT) and geographic longitude (GLONG) are shown.

remarkable height rise after local sunset on the disturbed day compared to the neighboring quiet days (Fig. 1b) indicates superposition of eastward electric field on the equatorial zonal field on this day. Fig. 2 shows the DMSP ion density plots around the initial phase of the storm. Though the passes do not exactly match the longitude of the observing station, prevailing postsunset ionospheric condition around the East Asian longitude sector may be portrayed. A flat-topped latitude variation of ion density is observed in Fig. 2a, while the latitudinal profile of ion density recorded irregular depletions/biteouts in Fig. 2b. Basu et al. (2002) reported equatorial scintillation events associated with flat-topped latitude variations of ion density. Ray et al. (2006) attempted to quantify the relation between the two considering 3 dB width of the flat-top. A threshold value of 24° for the 3 dB width was reported to correspond with higher occurrence probability of L-band (1.6 GHz) scintillation. In Fig. 2a the 3 dB width is estimated to be 27°. The flat-topped ionization distribution (Fig. 2a) may indicate that the equatorial ionization is uplifted to altitudes as high as the DMSP satellites (840 km). On the other hand, irregular depletions in the ion density profile (Fig. 2b) were identified by Young et al. (1984) to be associated with ESF. The ionosonde data of Trivandrum shows spread-F echoes in the ionograms after 1900 h IST (Fig. 3a–d) interrupting measurements of $h'F$ after 1930 h IST (Fig. 1b). All these features are assumed to be the results of enhanced eastward electric field at the magnetic equator during postsunset hours of magnetically disturbed days at the corresponding longitude zones.

From the location near the anomaly crest (Calcutta) strong equatorial scintillations (SI > 10 dB) were recorded in the paths of two satellites ETS-2 and FSC around 1930 h IST which continued till next morning. It may be mentioned that under quiet geomagnetic condition occurrence of scintillation at the present location is mainly equinoctial (February–April, August–October)

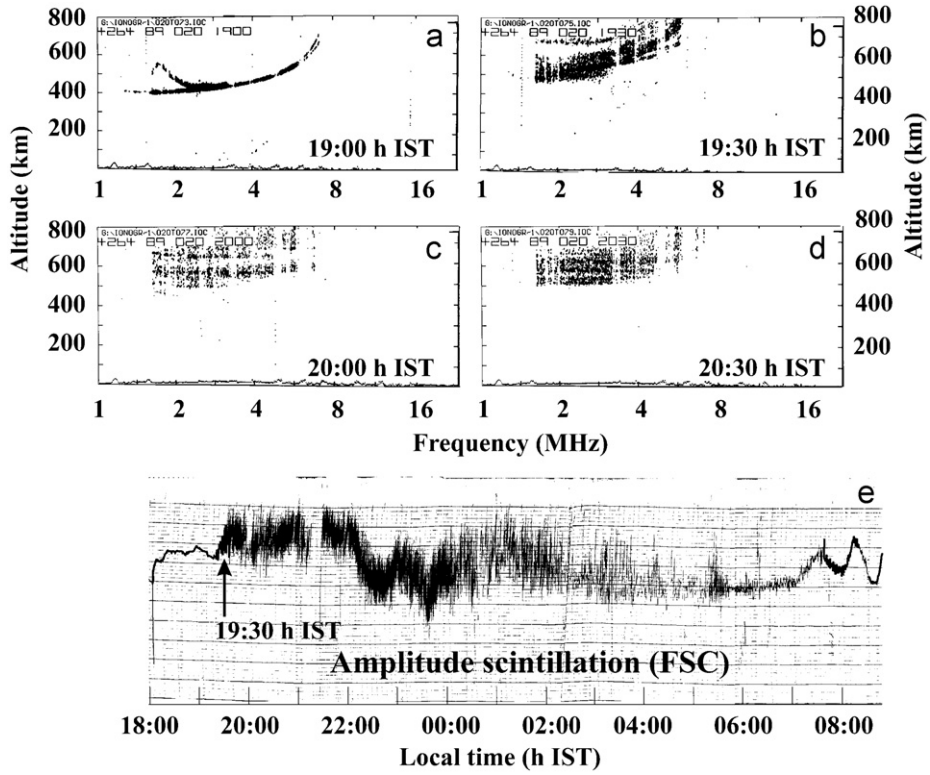

Fig. 3. Sample ionograms at (a) 1900 h LT, (b) 1930 h LT, (c) 2000 h LT and (d) 2030 h LT on January 20, 1989 over an equatorial station, Trivandrum. (e) A sample amplitude recording at UHF (244 MHz) signal from FSC showing postsunset scintillation on January 20, 1989. The data were recorded at Ionosphere Field Station, Haringhata, University of Calcutta.

and winter solstitial (November–January) phenomenon of high solar activity period (Chakraborty et al., 1999). About 15% post-sunset equatorial scintillation occurrence was recorded in the month of January, 1989. The eastward PRE electric field is the most important factor for generation of irregularities. It raises the F-layer to higher altitudes by $\boldsymbol{E}\times\boldsymbol{B}$ drift, where conditions favorable for generation of irregularities persist. It was reported that increase in the F-layer height and ESF onset during evening hours of quiet geomagnetic condition are well connected with EEJ ground strength before sunset (Uemoto et al., 2010). Under present investigation, triggering of ESF/scintillation during storm main phase due to modification of equatorial field by PP electric field of magnetospheric origin is evident in the variations of EEJ (Fig. 1a) and $h'F$ (Fig. 1b) in the postsunset period. The duration of scintillation event in the satellite path of FSC is shown in Fig. 1e by horizontal bar. The sample amplitude scintillation record at the UHF (244 MHz) frequency is also shown in Fig. 3e. Though the irregularity generation after the MPO is attributed to the modification of the equatorial electric field by PP effect, the continuation of the scintillation throughout the night – well inside main phase of the storm – may be related to the effects of DD which is effective within a few hours of storm onset. The polarity of DD electric field is eastward at the night (Abdu et al., 2007) that may perturb the normally prevailing nighttime westward electric field, leading to continuous evolution of irregularities throughout the night. The irregularities are mapped down along the magnetic field lines to the anomaly crest latitudes to produce scintillation. The scale sizes of the irregularities which are $\sim$1.2 km for ETS-2 and $\sim$800 m for FSC also play dominant roles to indicate longer duration scintillation, once triggered (Basu and Basu, 1981).

Unavailability of solar wind data makes the analysis somewhat incomplete in the context of solar wind parameters.

3.2. Storm on December 19, 1980

The geomagnetic storm on December 19, 1980, starts with SSC at 1026 h IST (Fig. 4). The main phase occurs, as indicated by abrupt decrease in D_{st} index, around 1730 h IST. It reaches minimum value of -240 nT around 2330 h IST on the same night (Fig. 4f). A sharp rate of decrease ~ -60 nT/h in D_{st} is noted around postsunset hours (1807 h IST being the local subionospheric sunset time). The time period is marked by a sharp increase in AE index that reaches the maximum value of 1641 nT at 2022 h IST (Fig. 4g). The IMF B_z turns strongly southward around 1800 h IST registering the lowest value of ~ -30 nT around 2030 h IST (Fig. 4d). All these signatures are reported to associate with penetration of eastward electric field at the equatorial latitudes in the postsunset period. As there is data gap for few hours in the horizontal component of geomagnetic field at Alibag (ΔH_A), the diurnal variations of magnetometer H-field data at the equatorial station, Trivandrum, (ΔH_T) and an off-equatorial station Ujjain (ΔH_U) (geographic: 23.18°N, 75.78°E) are shown (Fig. 4e). Compared to preceding/succeeding quiet days (as shown by mass plots) large unusual negative perturbations on the disturbed day around 1830 h IST are evident in the H-field variations of Trivandrum and Ujjain. This may signify the superposition of a large westward electric field of magnetospheric origin on the normal quiet time field pattern. The westward field during postsunset hours may suppress the upward $\boldsymbol{E}\times\boldsymbol{B}$ drift that is an important driver of irregularity generation at the magnetic equator responsible for ESF/scintillation. As a result, no equatorial scintillation was recorded from Calcutta. A sample record of amplitude signal from satellite ETS-2 during postsunset hours of December 19, 1980, indicates absence of scintillation (Fig. 5). It may be noted that on quiet days of December 1980 percentage occurrence of postsunset scintillation is estimated to be about

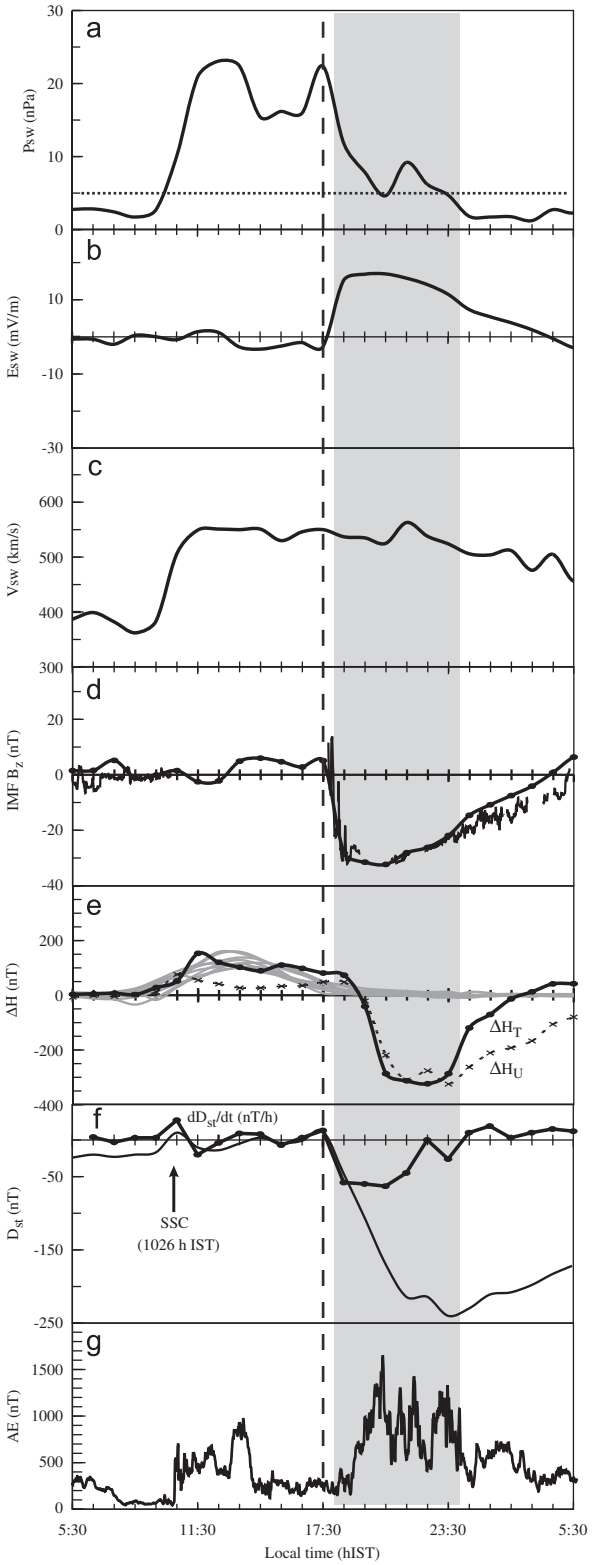

Fig. 4. Temporal variations of (a) P_{sw} (nPa), (b) IEF E_{sw} (mV/m), (c) V_{sw} (km/s), (d) IMF B_z (nT) at 1 min resolution, the filled circles connected by bold lines representing hourly average data, (e) magnetometer H-components at the equatorial station, Trivandrum, ΔH_T (nT) (filled circles connected with bold lines) and off-equatorial station Ujjain, ΔH_U (nT) (crosses connected with dotted lines) for the storm day along with mass plots ΔH_T for quiet days preceding and succeeding the storm day, (f) D_{st} index (nT) (continuous line) and dD_{st}/dt (nT/h) (filled circles connected with bold lines) (g) AE index (nT) for the storm event on December 19, 1980. The vertical dashed line represents the local time of MPO while local time of SSC is shown by a vertical arrow in panel (f). The shaded portion shows the time period after subionospheric sunset at ETS-2 satellite path till local midnight.

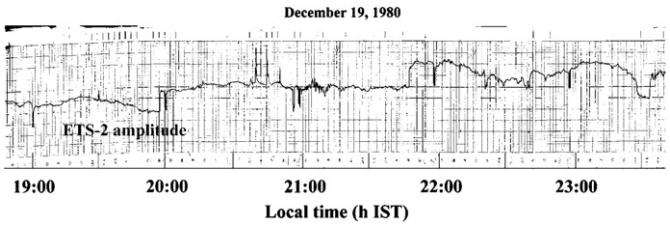

Fig. 5. Amplitude chart recording of VHF (136.11 MHz) signal from ETS-2 satellite showing no scintillation on December 19, 1980.

20% at the present location (Calcutta). PRE of eastward electric field, as stated earlier, is the primary factor for occurrence of density irregularities. Appearance of westward electric field, as revealed through the magnetometer data, may spoil the irregularity process on the disturbed day. Unfortunately no ionosonde data is available for this period.

Simultaneous investigation on solar wind data exhibits arrival of shock compression as revealed through sharp increases in P_{sw} from 1.7 to 23 nPa (Fig. 4a), V_{sw} from 360 to 550 km/s around 0930 h IST (Fig. 4c). The IEF E_{sw} shows a peak value $\sim$17 mV/m at 2030 h IST after which it decreases steadily (Fig. 4b). Although V_{sw} remains more or less constant during the onset of main phase (1730 h IST), P_{sw} decays rapidly during postsunset period.

3.3. Storm on February 6, 1981

An intense geomagnetic storm occurs with SSC at 1417 h IST on February 6, 1981 (Fig. 6). The main phase starts around 1830 h IST just before the local sunset ($\sim$1839 h IST). The onset of main phase is marked by a sharp decrease in SYM-H at the rate -33 nT/h (Fig. 6h). It exhibits maximum negative excursion of -153 nT at 0641 h IST on the next morning. IMF B_z exhibits a strong southward component (~ -15 nT) around the MPO time (Fig. 6d). AE also rises sharply and reaches a value of $\sim$2150 nT at 1950 h IST (Fig. 6i). ASY-H is seen to follow the trend of AE index (Fig. 6g). Observation of ionosonde data from the equatorial station, Kodaikanal, indicates interruption of $h'F$ measurement due to strong ESF after MPO during local sunset (Fig. 6f). Also, intense equatorial type scintillation ($SI_{dB} > 10$) was recorded at Calcutta in the path of ETS-2 from 2110 to 2300 h IST (inset Fig. 6f). Observation of EEJ for the event shows presence of noontime CEJ or westward electric field at the magnetic equator that strongly reverses to eastward direction ($\sim$28 nT) after MPO (Fig. 6e). It may be noted that the observed EEJ strength in the postsunset hours is much greater than quiet time CEJ conditions ($\sim$10 nT) (Hajra et al., 2009) and the field pattern on the day is totally different from the normal quiet time trend as shown by the mass plots. The coherent picture of sharp rise in AE/ASY-H, change in EEJ field and subsequent generation of ESF at the magnetic equator and equatorial scintillation observation near the anomaly crest may indicate the PP of high latitude electric field of eastward polarity to the equatorial latitude. The PP electric field may intensify the normally present eastward PRE electric field to lift the F-layer to higher altitudes where conditions favorable for generation of irregularities at the magnetic equator persist. These are manifested by the occurrences of ESF and scintillation near the anomaly crest location.

Simultaneous observation of solar wind parameters indicates the arrival of a magnetospheric shock compression around 1330 h IST when V_{sw} increase from 400 to 550 km/s (Fig. 6c) and P_{sw} from 1.5 to 14.5 nPa (Fig. 6a). Although a fall in P_{sw} is noted around the time of MPO, a large value ($P_{sw} > 5$ nPa) of shock compression

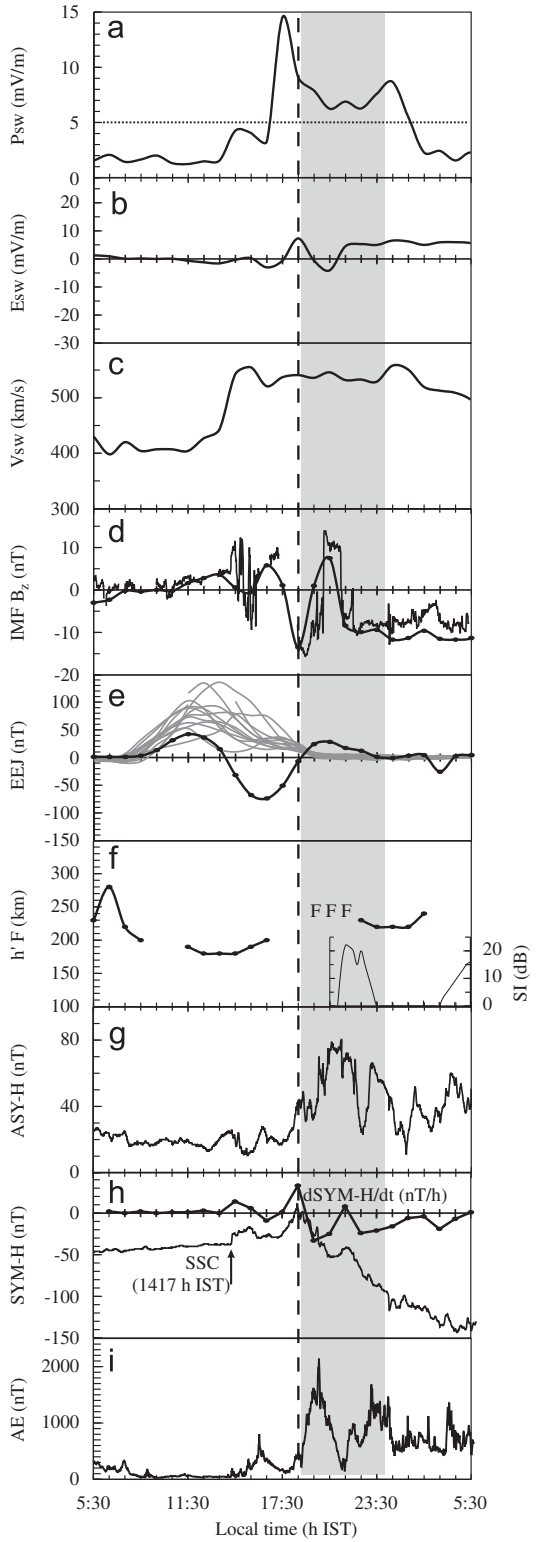

Fig. 6. Figures (a)–(d) are same as those in Fig. 4, but for the storm event on February 6, 1981. For this event the temporal variations of (e) EEJ (nT) for the storm day (filled circles connected with bold lines) along with mass plots for quiet days preceding and succeeding the storm day, (f) h'/F (km) at an equatorial station, Kodaikanal, (g) ASY-H (nT), (h) SYM-H (nT) (continuous line) and dSYM-H/dt (nT/h) (shown by filled circles connected with bold lines), (i) AE index (nT) are also shown. In the panel (f) "*F*" denotes the occurrence of ESF at Kodaikanal while the inset figure in the same panel shows temporal variation of scintillation index (SI) (dB) at 136.11 MHz.

persists for a long period. The continuation of a large value of V_{sw} is also evident in the plot. The shock compression reduces after 0030 h IST as indicated by sharp decrease in P_{sw} (~1 nPa).

3.4. Storm of July 25, 1981

Another very intense storm starts with the SSC at 1044 h IST on July 25, 1981 (Fig. 7). The MPO time is around 1850 h IST (local sunset time ~1936 h IST). In the main phase, SYM-H exhibits a sharp decrease at −68 nT/h around 1930 h IST and reaches minimum value of −256 nT at 0139 h IST (Fig. 7g). The occurrence of main phase is preceded by southward turning of IMF B_z around 1657 h IST and it remains southward for more than 6 h (Fig. 7d). AE also increases abruptly and reaches a value of ~3150 nT at 1850 h IST (Fig. 7h). A similar type of variation is observed for ASY-H index that attains a maximum of 300 nT at 1946 h IST (Fig. 7f). Unfortunately no magnetometer data is available for the day. The $h'F$ measurement is interrupted around the postsunset period due to presence of ESF at the equatorial station, Kodaikanal (Fig. 7e). From Calcutta severe equatorial scintillation is recorded in the path of ETS-2 from 1900 h IST till 0115 h IST (inset Fig. 7e). Presence of ESF at the magnetic equator and scintillation near the anomaly crest may be caused by strengthening of PRE by the PP of eastward electric field around the local dusk hours. For the presence of equatorial irregularity throughout the premidnight, the dominance of eastward DD electric field over the normally prevailing nighttime westward electric field may be one of the probable causes. Further, Huang (2008) showed that eastward penetration electric field in the dusk sector may last about 10 h without effective shielding when the magnetic storm activity is strengthening (storm main phase) during continuous southward IMF B_z.

It may be noted that under quiet geomagnetic condition, the nature of summer solstitial scintillation mostly differs from that of the equatorial type scintillation. The percentage occurrence of postsunset scintillation for the month of July 1981 is estimated to be about 10% during magnetically quiet periods. The locally generated or E-region irregularities are mainly responsible for summer type scintillation contrary to the equatorial scintillation for which F-region irregularities are mainly responsible. F-region scintillation is generally quite fast and saturates within a few minutes. E-region scintillation is slowly varying with quasi-periodic fluctuations at the beginning/start and end. The initiation of severe scintillation in the present case (during storm main phase) is related to the equatorial field modifications by PP electric field of magnetospheric origin.

Solar wind parameters for the event indicate a multi-step shock development initiating primarily around 0930 h IST that strengthens further at 1730 h IST. V_{sw} increases from ~400 to 800 km/s (Fig. 7c) and P_{sw} from 2 to 26 nPa (Fig. 7a). The sustenance of the large shock compression (>5 nPa) for a long period in the local postsunset period is evident in the plots.

3.5. Storm of November 27, 1990

Following the SSC at 0502 h IST, the main phase of the intense storm starts around 1858 h IST on November 27, 1990 (local sunset time ~1802 h IST) (Fig. 8). A large rate of decrease in SYM-H (~−50 nT/h) is noted in the postsunset period (Fig. 8h). Following a two-step growth of ring current, SYM-H index reaches its minimum value of −157 nT at 0252 h IST. Strong southward component of IMF B_z (>-10 nT) is recorded during the entire period of main phase (Fig. 8d). AE exhibits gradual increase and reaches the maximum value of ~2550 nT around 2200 h IST (Fig. 8i). ASY-H attains its maximum value (~180 nT) around 2240 h IST (Fig. 8g). The diurnal variation of EEJ shows unusual, compared to the magnetically quiet day patterns, downward perturbation in the postsunset period (Fig. 8e). The $h'F$ data of equatorial station, Kodaikanal, exhibit lower values on the disturbed day compared

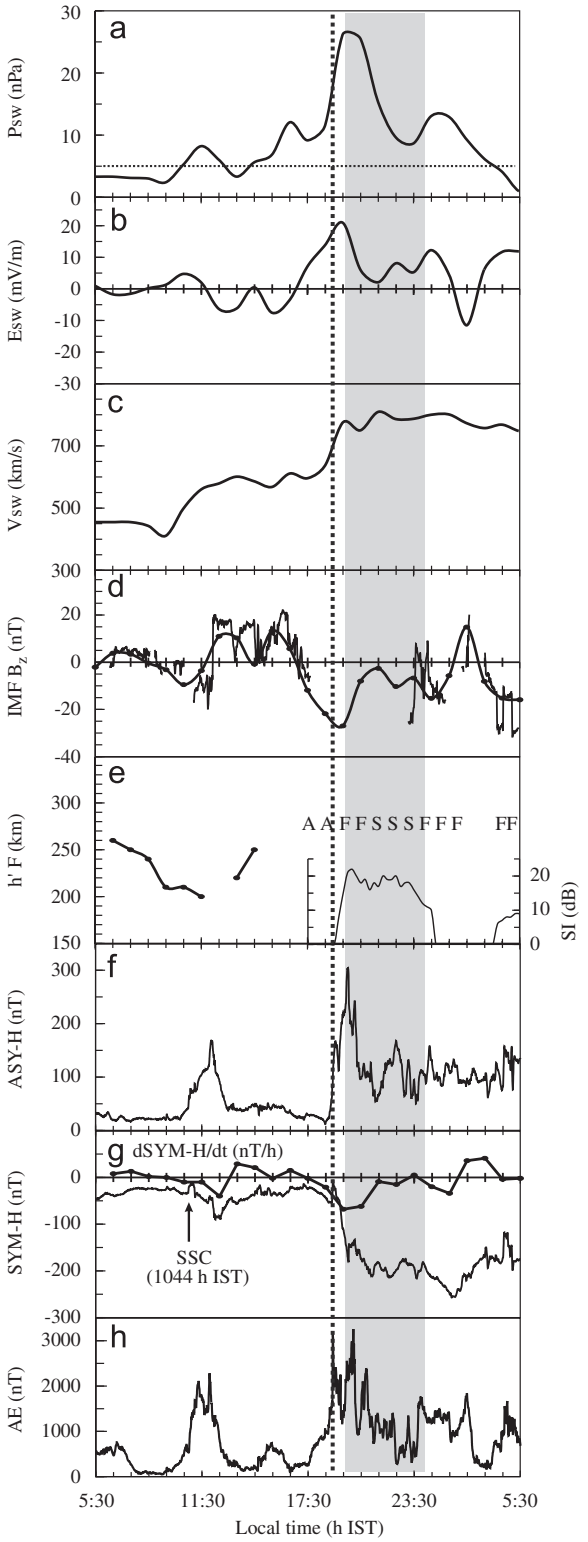

Fig. 7. Figures (a)–(d) are same as those in Fig. 4, (e)–(h) are same as (f)–(i) in Fig. 6, but for the storm event commencing on July 25, 1981. In panel (e) temporal variation of $h'F$ (km) are shown where "*A*" and "*S*" indicate measurements influenced by, or impossible because of the presence of a lower thin layer, e.g., E_s and interference/atmospherics respectively while "*F*" denotes the occurrence of ESF at Kodaikanal.

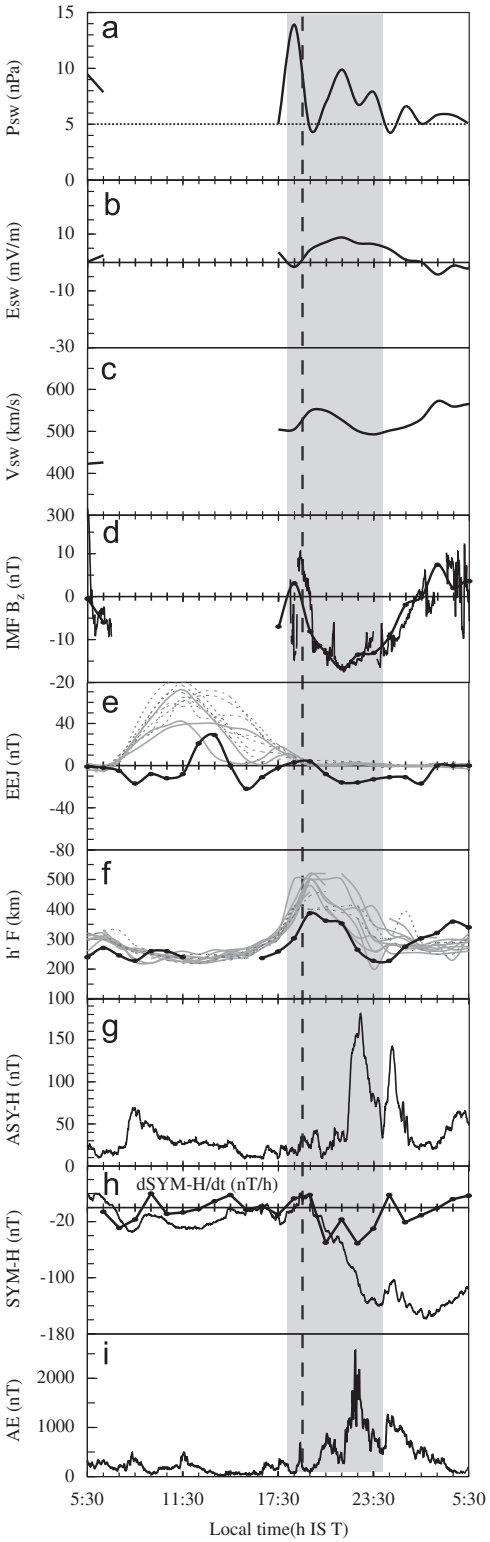

Fig. 8. Same as Fig. 6, but for the storm event commencing on November 27, 1990. In panels (e) and (f) the continuous and dotted lines pertain to quiet days with and without scintillation event, respectively.

to magnetically quiet days with or without scintillation (Fig. 8f). DMSP ion density distribution (Fig. 9) also confirms the absence of anomaly during the local dusk period from the Indian longitude sector. While the signature of a peak with comparatively less 3 dB width ($\sim 17^{\circ}$) may be noted in Fig. 9a, such peak is conspicuously absent in Fig. 9b. The absence of any anomaly structure at the satellite heights is consistent with the downward electric field perturbation at the magnetic equator as indicated by EEJ variation. No scintillation was recorded in the paths of the satellites ETS-2 and FSC during postsunset period, though under quiet geomagnetic

condition, the percentage occurrence of postsunset scintillation is recorded to be about 48% in the month of November, 1990. Ionogram data from Trivandrum also shows no signature of spread echoes during the local dusk sector (Fig. 10). Non-occurrence of irregularities may be related to equatorial field modification, which is reflected in the variations of EEJ (Fig. 8e) and $h'F$ (Fig. 8f).

The solar wind data for this event is not continuous (Fig. 8a–c). Though the arrival time of magnetospheric shock compression is not clear from the plot, an abrupt decrease in P_{sw} from 14 nPa to a value less than 5 nPa around 1930 h IST in the main phase is evident in Fig. 8a.

4. Discussion

The results of case studies on the ionospheric responses in the main phases of geomagnetic storms, initiating around local dusk sector, may be discussed in the context of polarity of PP electric field and subsequent generation/inhibition of ESF/scintillation. The PP of electric field depends on the magnetospheric dynamo, which converts solar wind energy into electromagnetic energy in the magnetosphere via reconnection process between the solar wind and earth's magnetic fields. The nature of this reconnection is suggested to depend strongly on the direction of the IMF (Rastogi and Patel, 1975; Gonzales et al., 1979; Kelley et al., 1979). The magnetosphere intercepts, on the average, 10–20% of the solar wind voltage across its diameter. When this voltage is impressed onto the ionosphere it becomes high latitude polar cap potential, sudden changes of which lead to the PP effect.

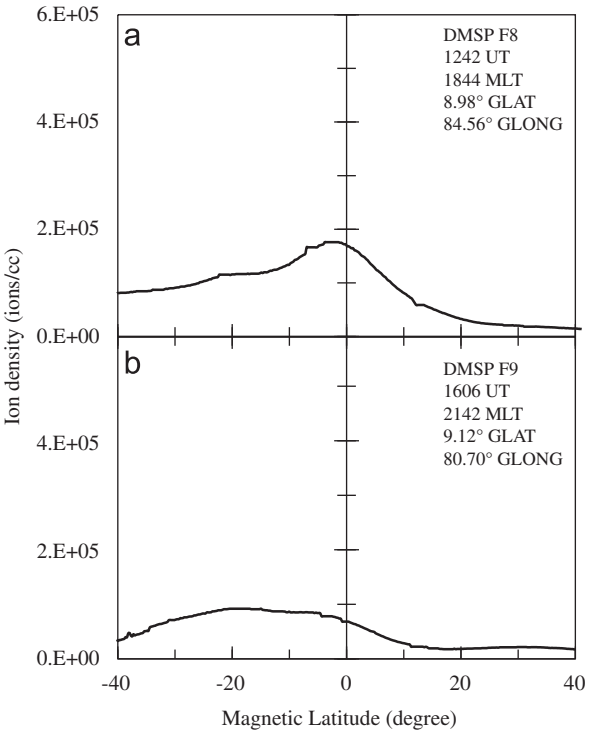

Fig. 9. Same as Fig. 2, but for the storm event on November 27, 1990.

In the main phase of storms initiating around local sunset hours, the eastward perturbation of the equatorial zonal electric field by PP effect was reported in association with abrupt increases in AE index (Fejer and Scherliess, 1995, 1997) and ASY-H index (Sastri et al., 1997). Basu et al. (2001, 2010) developed a scheme to specify the longitude sector within the low latitude ionosphere which is most susceptible to storm related plasma bubble and scintillation activity due to PP eastward electric field. Accordingly, during the main phase of intense magnetic storms plasma bubbles/scintillations are most likely to occur at the specific longitude sectors for which the universal time interval between the rate of change of $D_{st} \leq -50$ nT/h and the D_{st} minimum ≤ -100 nT corresponds to the period of local dusk.

The present study reveals that for the storm on February 6, 1981 (event 3.3, Fig. 6), SYM-H exhibits a sharp decrease of -33 nT/h during local postsunset hours while much sharper rates of decrease, -84 and -68 nT/h, during the local dusk sector are recorded for the events on January 20, 1989 (3.1, Fig. 1) and July 25, 1981, (3.4, Fig. 7) respectively. During the same period large southward IMF B_z values and sharp increases in AE index are noted for two cases (3.3, Fig. 6 and 3.4, Fig. 7). Also ASY-H index registers sharp increases for the three events around the postsunset period. While the EEJ data is not available for the event 3.4 (Fig. 7), diurnal variations of EEJ in cases of the events 3.1 (Fig. 1) and 3.3 (Fig. 6) exhibit signature of superposition of eastward electric field on the local dusk time zonal field. For all the events ESF is recorded at the equatorial station, Kodaikanal/Trivandrum, and strong equatorial scintillation is noted in the path of ETS-2/FSC from Calcutta, situated near the northern crest of EIA. For the event 3.1, flat-topped structure and irregular fluctuations extending throughout the crests are noted in the ion density distribution as measured by consecutive passes of DMSP satellites in the East Asian longitude sector (Fig. 2). These may be the

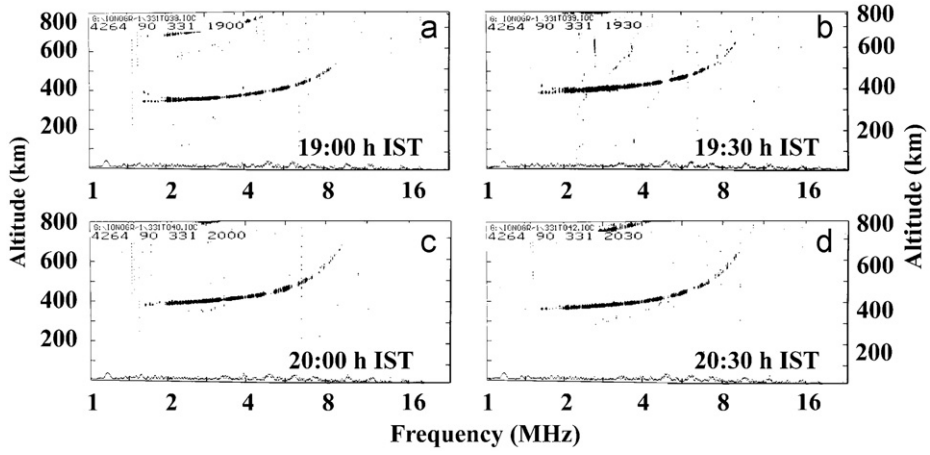

Fig. 10. Ionograms showing absence of ESF in the postsunset period over an equatorial station, Trivandrum for the storm event of November 27, 1990.

signatures of strengthening of eastward electric field at the magnetic equator in the dusk sector by the action of eastward PP electric field.

After local sunset, abrupt decreases in D_{st}/SYM-H at the rates -60 nT/h and -50 nT/h are observed for the events on December 19, 1980 (3.2, Fig. 4) and November 27, 1990 (3.5, Fig. 8), respectively. In both the cases storm onset (MPO) is preceded by strong southward turning of IMF B_z and the same phase is maintained throughout the main phases. For the event 3.2 (Fig. 4), a sharp increase in AE is detected, while steady increase in AE is recorded for event 3.5 (Fig. 8). In both the cases signatures of westward field perturbations are reflected in the variations of ΔH/EEJ and no scintillation is recorded around local postsunset period in the path of ETS-2 or FSC. In spite of prevailing all the conditions, i.e., (i) large rates of decreases in D_{st}/SYM-H index in the local dusk sector, (ii) abrupt southward turning of IMF B_z along with its continuation of the state for long period and (iii) sharp increase in AE during local dusk – suggested to be suitable proxies for penetration of eastward electric field to the equatorial latitudes – signatures of westward PP are reflected in the two cases. Thus abrupt changes of the parameters may not always be accepted to be the indices of the penetration of eastward electric field and evolution of postsunset irregularities. This fact instincts investigations of the solar wind data for identification of better indices in the context of polarity of PP electric field and subsequent generation of irregularities.

The solar wind control of the equatorial electric field is a long-studied topic (Kelley et al., 1979, and references therein; Sazykin et al., 2004). According to Kelley et al. (1979), large scale rapid change in magnetospheric convection associated with variation of solar wind parameters is the key factor for the equatorial electric field perturbation during rapid reversal of IMF B_z. During the storm period ($K_p > \sim 3$) of high solar activity years a direct linkage between the equatorial electric field and the IEF due to the dominance of solar wind sources was suggested by Earle and Kelley (1987). Analyzing a number of storm events Martinis et al. (2005) inferred that during the main phase of a storm an enhanced value of E_{sw}, in the range 5–15 mV/m, may be taken as the threshold for the generation of postsunset ESF associated with PP of eastward electric field.

For the present investigation solar wind data are available for four events – two (3.3, Fig. 6 and 3.4, Fig. 7) are associated with postsunset ESF/scintillation, while the other two (3.2, Fig. 4 and 3.5, Fig. 8) are exempted from ESF/scintillation event. The major solar wind/interplanetary parameters after MPO around the local sunset hours for each of the storm events are presented in Table 1. A close scrutiny of the table reveals that the magnitudes of the solar wind/interplanetary parameters, as reported earlier, are not always effective indices for postsunset penetration of eastward electric field and subsequent occurrence of ESF/scintillation from the present longitude sector. For example, in spite of high $E_{sw} \sim 17$ mV/m no scintillation is detected for the event 3.2, while it occurs for event 3.3 when $E_{sw} \sim 4$ mV/m. On the contrary, a comparative study of these two groups of events reveals that local time of arrival and sustenance of magnetospheric shock compression during local sunset-to-post-sunset period may be treated as important precursor for penetration of eastward electric field to the equatorial and low latitude zone. For the storm event on February 6, 1981 (3.3, Fig. 6) with MPO around 1830 h IST the magnetospheric shock compression – as indicated by abrupt increases in P_{sw}, V_{sw} – arrives at 1330 h IST and a further intensification occurs around 1630 h IST followed by sustenance of large value of P_{sw} (> 5 nPa) for a long period ($>$ 6 h). For the event on July 25, 1981 (3.4, Fig. 7) strengthening of the shock compression around 1730 h IST before the MPO ($\sim$1850 h IST) is also evident and the large value of P_{sw} ($>$ 5 nPa) continued for several hours ($>$ 7 h).

The solar wind–magnetosphere–ionosphere coupling is modulated significantly by P_{sw} variations in addition to changes in the IMF (Boudouridis et al., 2007, and references therein). Gonzalez et al. (1989) suggested the best solar wind–magnetospheric coupling function to vary with $P_{sw}^{1/2}V_{sw}B_z$, thus inferring increase in magnetospheric reconnection power with the enhancement of P_{sw}. Numerous studies during the last decade (Zesta et al., 2000; Shue and Kamide, 2001; Boudouridis et al., 2003; Lee et al., 2004; Palmroth et al., 2004) confirm enhanced "geoeffectiveness" of solar wind and increase in "coupling efficiency" between the solar wind and the magnetosphere due to sudden increase in P_{sw} under the condition of southward IMF B_z. These are revealed through the effects like intensification of magnetospheric and ionospheric currents, enhanced energy flux deposition in auroral ionosphere, increase in high latitude Joule heating, etc. The sharp increase in solar wind pressure shrinks the magnetosphere—the magnetopause and cross-tail current sheet move closer to the earth with increases in corresponding currents (Wing and Sibeck, 1997; Clauer et al., 2001, and references therein). The enhanced reconnection in the magnetotail driven by the compression of the magnetosphere generates excess closed magnetic field lines in the polar cap (Boudouridis et al., 2004; Prolss, 2004). As a result, the polar cap potential directed from dawn-to-dusk increases abruptly. Rapid increase in polar cap potential produces sudden enhancement in higher-latitude auroral current system (Region 1 current). In the magnetosphere–ionosphere coupling process, the Region 1 current associated with the maximum possible ionospheric convection potential (Hill et al., 1976) is expressed analytically to increase non-linearly with P_{sw} (Siscoe et al., 2002) as follows:

$$I_s = 4.6 {P_{sw}}^{1/3} D^{1/3}$$

where I_s is expressed in MA, P_{sw} in nPa and D is normalized dipole strength of the earth. While the Region 1 current increases promptly following the rapid increase in polar cap potential by P_{sw} impulse, the Region 2 current (lower-latitude current system in auroral region), which shields the mid- and equatorial-latitudes from the high latitude electric fields, cannot change at the same rate. The imbalance situation, known as "undershielding condition", leads to PP of electric fields to low latitudes, the polarity of which is eastward around local postsunset period. It strengthens the eastward PRE electric field. The enhanced

Table 1
Values of solar wind/interplanetary parameters around local sunset period for the storm events.

Event	Date	IMF B_z (nT)	E_{sw} (mV/m)	V_{sw} (km/s)	P_{sw} (nPa)	ΔT (min)[a]	Scintillation occurrence
3.2	December 19, 1980	−32	17	550	22	85	No
3.3	February 6, 1981	−14	4	546	9	411	Yes
3.4	July 25, 1981	−27	14	775	26	474	Yes
3.5	November 27, 1990	−17	9	549	7	<60	No

[a] *Note*: "ΔT" indicates the time period (in min) of sustenance of magnetospheric shock compression as indicated by large values of P_{sw} (>5 nPa) around local sunset time.

eastward electric field at the magnetic equator may uplift the F-layer to high altitudes where (i) collision frequency between ions and electrons is less and (ii) the effects of local chemical recombination of major ionic species are negligible. The situation is conducive for generation of irregularities through the mechanism of Rayleigh–Taylor instability during the period (Sultan, 1996, and references therein). It may be noted that in both the cases (events 3.3 and 3.4) the shock magnitude reduces ($P_{sw} < 5$ nPa) around local postmidnight-to-dawn sector.

For the other two events – storms during December 19, 1980 (3.2, Fig. 4) and November 27, 1990 (3.5, Fig. 8) – abrupt decreases in P_{sw} around 1730 h IST and 1830 h IST respectively are followed by fluctuations around 5 nPa confirming less durations (1–1.5 h) of shock compression around sunset/postsunset period. It may signify the sudden reduction in magnetospheric convection and/ polar cap potential leading to quick decrease in Region 1 current while Region 2 current remains large. This results in another imbalance situation known as "overshielding condition" that is also broken by the penetration of auroral region electric field instantaneously to the equatorial latitudes. The overshielding PP electric field has polarity (westward around local postsunset period) opposite to that due to undershielding since Region 2 current circulates in a sense opposite to Region 1 current. The westward electric field of PP origin along with DD electric field of same polarity, if at all appears, may weaken the PRE leading to non-occurrence of ESF/scintillation.

5. Conclusions

During the main phase of intense geomagnetic storms abrupt increases in AE, ASY-H and/or decrease in D_{st}/SYM-H under the condition of strong southward component of IMF B_z may indicate penetration of eastward electric field to the equatorial latitude around local dusk period leading to evolution of plasma density irregularities if the time period is associated with arrival and sustenance of appreciably large magnitude ($P_{sw} > 5$ nPa) shock compression for 6 or more hours. The inhibition of postsunset equatorial scintillation due to penetration of westward electric field may be more feasible if the magnetospheric shock reduces suddenly or fluctuates with small values ($P_{sw} < 5$ nPa) resulting in sustenance of the shock for short period (1–1.5 h) after local subionospheric sunset.

An abrupt enhancement in solar wind pressure in the dusk sector followed by sustenance of large magnitude shock ($P_{sw} > 5$ nPa) under the condition of southward IMF B_z may be suggested to be efficient indicator for solar wind–magnetospheric coupling leading to penetration of eastward electric fields to the equatorial latitudes and consequent generation of postsunset density irregularities. It may be noted that the present observation is based on four/five storm events with MPO around the local sunset period. For any bold suggestion in this respect more case studies concerning the solar wind–magnetosphere–ionosphere coupling are needed.

Acknowledgments

Authors are greatly indebted to Prof. A. DasGupta, University of Calcutta, for supplying amplitude scintillation data, and for useful discussions and valuable suggestions. The authors are thankful to Indian Institute of Geomagnetism, Mumbai, for providing magnetometer data, to Prof. J.H. Sastri, Indian Institute of Astrophysics, Bangalore, for providing ionosonde dada and to Dr. Sudha Ravindran, Space Physics Laboratory, Trivandrum, for supplying ionograms for two events. Authors are also thankful to Marc Hariston, Utdallas, for providing DMSP ion density data. The work has been carried out with the financial assistance of ISRO under the RESPOND Program.

References

Aarons, J., Mullen, J.P., Koster, J.P., da Silva, R.F., Medeiros, J.R., Medeiros, R.T., Bushby, A., Pantoja, J., Lanat, J., Paulson, M.R., 1980. Seasonal and geomagnetic control of equatorial scintillations in two longitudinal sectors. Journal of Atmospheric and Terrestrial Physics 42, 861–866.

Abdu, M.A., Batista, I.S., Takahashi, H., MacDougall, J., Sobral, J.H., Medeiros, A.F., Trivedi, N.B., 2003. Magnetospheric disturbance induced equatorial plasma bubble development and dynamics: a case study in Brazilian sector. Journal of Geophysical Research 108, 1449. doi:10.1029/2002JA009721.

Abdu, M.A., Maruyama, T., Batista, I.S., Saito, S., Nakamura, M., 2007. Ionospheric response to the October 2003 superstorm: longitude/local time effects over equatorial low and middle latitudes. Journal of Geophysical Research 112, A10306. doi:10.1029/2006JA012228.

Alex, S., Rastogi, R.G., 1987. Geomagnetic disturbance effects on equatorial spread F. Annales Geophysicae 5, 83–88.

Basu, S., Basu, Su., 1981. Equatorial scintillation—a review. Journal of Atmospheric and Terrestrial Physics 43, 473–489.

Basu, Su., Basu, S., Valladares, C.E., Yeh, H.C., Su, S.Y., MacKenzie, E., Sultan, P.J., Aarons, J., Rich, F.J., Doherty, P., Groves, K.M., Bullett, T.W., 2001. Ionospheric effects of major magnetic storms during the interplanetary space weather period of September and October 1999: GPS observations, VHF/UHF scintillations, and in situ density structures at middle and equatorial latitudes. Journal of Geophysical Research 106, 30389–30413.

Basu, S., Groves, K.M., Basu, Su., Sultan, P.J., 2002. Specification and forecasting of scintillations in communication/navigation links: current status and future plans. Journal of Atmospheric Solar–Terrestrial Physics 64, 1745–1754.

Basu, S., Basu, Su., MacKenzie, E., Bridgwood, C., Valladares, C.E., Groves, K.M., Carrano, C., 2010. Specification of the occurrence of equatorial ionospheric scintillations during the main phase of large magnetic storms within solar cycle 23. Radio Science 45, RS5009. doi:10.1029/2009RS004343.

Becker-Guedes, F., Sahai, Y., Fagundes, P.R., Lima, W.L.C., Pillat, V.G., Abalde, R., Bittencourt, J.A., 2004. Geomagnetic storm and equatorial spread-F. Annales Geophysicae 22, 3231–3239.

Blanc, M., Richmond, A.D., 1980. The ionospheric disturbance dynamo. Journal of Geophysical Research 85, 1669–1686.

Booker, H.G., Wells, H.W., 1938. Scattering of radio waves by the F region of the ionosphere. Journal of Geophysical Research 43, 249–256.

Boudouridis, A., Zests, E., Lyons, L.R., Anderson, P.C., Lummerzheim, D., 2003. Effect of solar wind pressure pulses on the size and strength of the auroral oval. Journal of Geophysical Research 108, 8012. doi:10.1029/2002JA009373.

Boudouridis, A., Zesta, E., Lyons, L.R., Anderson, P.C., Lummerzheim, D., 2004. Magnetospheric reconnection driven by solar wind pressure fronts. Annales Geophysicae 22, 1367–1378.

Boudouridis, A., Lyons, L.R., Zesta, E., Ruohoniemi, J.M., 2007. Dayside reconnection enhancement resulting from a solar wind dynamic pressure increase. Journal of Geophysical Research 112, A06201. doi:10.1029/2006JA012141.

Chakraborty, S.K., DasGupta, A., Ray, S., Banerjee, S., 1999. Long-term observations of VHF scintillation and total electron content near the crest of the equatorial anomaly in the Indian longitude zone. Radio Science 34, 241–255.

Chandra, H., Rastogi, R.G., 1974. Geomagnetic storm effects on ionospheric drifts and the equatorial E_s over the magnetic equator. Indian Journal of Radio and Space Physics 3, 332–336.

Clauer, C.R., Alexeev, I.I., Belenkaya, E.S., Baker, J.B., 2001. Special features of September 24–27, 1998 storm during high solar wind dynamic pressure and northward interplanetary magnetic field. Journal of Geophysical Research 106, 25695–25711.

Clauer, C.R., McPherron, R.L., 1980. The relative importance of the interplanetary electric field and magnetospheric substorm on the partial ring current development. Journal of Geophysical Research 85, 6747–6759.

Cohen, R., Bowles, K.L., 1961. On the nature of equatorial spread F. Journal of Geophysical Research 66, 1081–1106.

Earle, G.D., Kelley, M.C., 1987. Spectral studies of the sources of ionospheric electric fields. Journal of Geophysical Research 92, 213–224.

Farley, D.T., Balsley, B.B., Woodman, R.F., McClure, J.P., 1970. Equatorial spread F: implications of VHF radio observations. Journal of Geophysical Research 75, 7199–7216.

Fejer, B.G., Scherliess, L., 1995. Time dependent response of equatorial ionospheric electric fields to magnetospheric disturbances. Geophysical Research Letters 22, 851–854.

Fejer, B.G., Scherliess, L., 1997. Empirical models of storm time equatorial zonal electric fields. Journal of Geophysical Research 102, 24047–24056.

Gonzales, C.A., Kelley, M.C., Fejer, B.G., Vickrey, J.F., Woodman, R.F., 1979. Equatorial electric fields during magnetically disturbed conditions 2. Implications of simultaneous auroral and equatorial measurements. Journal of Geophysical Research 84, 5803–5812.

Gonzalez, W.D., Tsurutani, B.T., Gonzalez, A.L.C., Smith, E.J., Tang, F., Akasof, S.I., 1989. Solar wind–magnetosphere coupling during intense magnetic storms (1978-1979). Journal of Geophysical Research 94, 8835–8851.

Hajra, R., Chakraborty, S.K., DasGupta, A., 2010. Ionospheric effects near the magnetic equator and the anomaly crest of the Indian longitude zone during

a large number of intense geomagnetic storms. Journal of Atmospheric and Solar–Terrestrial Physics 72, 1299–1308.
Hajra, R., Chakraborty, S.K., Paul, A., 2009. Electrodynamical control of the ambient ionization near the equatorial anomaly crest in the Indian zone during counter electrojet days. Radio Science 44 (RS3009). doi:10.1029/2008RS003904.
Hill, T.W., Dessler, A.J., Wolf, R.A., 1976. Mercury and Mars: the role of ionospheric conductivity in the acceleration of magnetospheric particles. Geophysical Research Letters 3, 429–432.
Huang, C.S., 2008. Continuous penetration of the interplanetary electric field to the equatorial ionosphere over eight hours during intense geomagnetic storms. Journal of Geophysical Research 113, A11305. doi:10.1029/2008JA013588.
Huang, C.Y., Burke, W., Machuzak, J., Gentile, L., Sultan, P.J., 2002. Equatorial plasma bubbles observed by DMSP satellites during a full solar cycle: toward a global climatology. Journal of Geophysical Research 107 (1434). doi:10.1029/2002JA009452.
Jaggi, R.K., Wolf, R.A., 1973. Self-consistent calculation of the motion of a sheet of ions in the magnetosphere. Journal of Geophysical Research 78, 2852–2866.
Kelley, M.C., Fejer, B.G., Gonzales, C.A., 1979. An explanation for anomalous equatorial ionospheric electric fields associated with a northward turning of the interplanetary magnetic field. Geophysical Research Letters 6, 301–304.
Kil, H., Paxton, L.J., Oh, S.J., 2009. Global bubble distribution seen from ROCSAT-1 and its association with the evening prereversal enhancement. Journal of Geophysical Research 114, A06307. doi:10.1029/2008JA013672.
Knight, M., Finn, A., 1996. The impact of ionospheric scintillations on GPS performance. In: Proceedings of the Ninth International Technical Meeting of the Satellite Division of the Institute of Navigation (ION GPS 1996), Kansas City, MO, September 1996, pp. 555–564.
Kumar, S., Chandra, H., Sharma, S., 2005. Geomagnetic storms and their ionospheric effects observed at the equatorial anomaly crest in the Indian region. Journal of Atmospheric and Solar–Terrestrial Physics 67, 581–594.
Lee, D.Y., Lyons, L.R., Yumoto, K., 2004. Sawtooth oscillations directly driven by solar wind dynamic pressure enhancements. Journal of Geophysical Research 109, A04202. doi:10.1029/2003JA010246.
Mannucci, A.J., Tsurutani, B.T., Abdu, M.A., Gonzalez, W.D., Komjathy, A., Echer, E., Iijima, B.A., Crowley, G., Anderson, D., 2008. Superposed epoch analysis of the dayside ionospheric response to four intense geomagnetic storms. Journal of Geophysical Research 113 (A00A02). doi:10.1029/2007JA012732.
Martinis, C.R., Mendillo, M.J., Aarons, J., 2005. Toward a synthesis of equatorial spread F onset and suppression during geomagnetic storms. Journal of Geophysical Research 110, A07306. doi:10.1029/2003JA010362.
Maruyama, N., Richmond, A.D., Fuller-Rowell, T.J., Codrescu, M.V., Sazykin, S., Toffoletto, F.R., Spiro, R.W., Millward, G.H., 2005. Interaction between direct penetration and disturbance dynamo electric fields in the storm-time equatorial ionosphere. Geophysical Research Letters 32, L17105. doi:10.1029/2005GL023763.
Palmroth, M., Pilkkinen, T.I., Janhunen, P., McComas, D.J., Smith, C.W., Koskinen, H.E.J., 2004. Role of solar wind dynamic pressure in driving ionospheric Joule heating. Journal of Geophysical Research 109, A11302. doi:10.1029/2004JA010529.
Prolss, G.W., 2004. Origin of Birkeland currents, Physics of the Earth's Space Environment: An Introduction. Springer-Verlag, Berlin Heidelberg, Germany 390-395.
Rastogi, R.G., Patel, V., 1975. Effect of interplanetary magnetic field on ionosphere over the magnetic equator. Proceedings of Indian Academy of Science 82, 121–141.
Ray, S., Paul, A., DasGupta, A., 2006. Equatorial scintillations in relation to the development of ionization anomaly. Annales Geophysicae 24, 1429–1442.
Sastri, J.H., Abdu, M.A., Sobral, J.H.A., 1997. Response of equatorial ionosphere to episodes of asymmetric ring current activity. Annales Geophysicae 15, 1316–1323.
Sazykin, S., Wolf, R.A., Fejer, B.G., Spiro, R., de Zeeuw, D.L., Gombosi, T.I., Caldwell, J., 2004. Ionospheric prompt penetration electric fields: comparison of first-principle solutions with observations. American Geophysical Union, Fall Meeting 2004, Abstract SM54A-03.
Senior, C., Blanc, M., 1984. On the control of magnetospheric convection by the spatial distribution of ionospheric conductivities. Journal of Geophysical Research 89, 261–284.
Shue, J.H., Kamide, Y., 2001. Effects of solar wind density on auroral electrojets. Geophysical Research Letters 28, 2181–2184.
Siscoe, G.L., Erickson, G.M., Sonnerup, B.U.O., Maynard, N.C., Schoendorf, J.A., Siebert, K.D., Weimer, D.R., White, W.W., Wilson, G.R., 2002. Hill model of transpolar potential saturation: comparisons with MHD simulations. Journal of Geophysical Research 107, 1075. doi:10.1029/2001JA000109.
Spiro, R.W., Wolf, R.A., Fejer, B.G., 1988. Penetration of high-latitude-electric-field effects to low latitudes during SUNDIAL 1984. Annales Geophysicae 6, 39–50.
Sultan, P.J., 1996. Linear theory and modeling of the Rayleigh–Taylor instability leading to the occurrence of equatorial spread F. Journal of Geophysical Research 101, 26875–26891.
Tulasi Ram, S., Rama Rao, P.V.S., Prasad, D.S.V.V.D., Niranjan, K., Gopi Krishna, S., Sridharan, R., Rabindran, S., 2008. Local time dependent response of post-sunset ESF during geomagnetic storms. Journal of Geophysical Research 113, A07310. doi:10.1029/2007JA012922.
Uemoto, J., Maruyama, T., Saito, S., Ishii, M., Yoshimura, R., 2010. Relationships between PRE-sunset electrojet strength, PRE-reversal enhancement and equatorial spread-F onset. Annales Geophysicae 28, 449–454.
Wing, S., Sibeck, D.G., 1997. Effects of interplanetary magnetic field z component and the solar wind dynamic pressure on the geosynchronous magnetic field. Journal of Geophysical Research 102, 7207–7216.
Woodman, R.F., LaHoz, C., 1976. Radar observations of F region equatorial irregularities. Journal of Geophysical Research 81, 5447–5466.
Young, E.R., Burke, W.J., Rich, F.J., Sagalyn, R.C., 1984. The distribution of topside spread F from in situ measurements of Defense Meteorological Satellite Program: F2 and F4. Journal of Geophysical Research 89, 5565–5574.
Zesta, E., Singer, H.J., Lummerzheim, D., Russel, C.T., Lyons, L.R., Brittnacher, M.J., 2000. The effect of the January 10, 1997 pressure pulse on the magneto-sphere–ionosphere current system. In magnetospheric current systems. In: Ohtani, S., Fujji, R., Hesse, M., Lysak, R.L. (Eds.), Geophysical Monograph Series, 118. AGU, Washington, D.C, pp. 217–226.